

## Photo-orientation of liquid crystals due to light-induced desorption and adsorption of dye molecules on an aligning surface

E. Ouskova,<sup>1</sup> Yu. Reznikov,<sup>1,2</sup> S.V. Shiyonovskii,<sup>2,3</sup> L. Su,<sup>2</sup> J.L. West,<sup>2</sup> O.V. Kuksenok,<sup>3</sup> O. Francescangeli,<sup>4</sup> and F. Simoni<sup>4</sup>

<sup>1</sup>*Institute of Physics, 46 Prospect Nauki, Kyiv, 03039, Ukraine*

<sup>2</sup>*Liquid Crystal Institute, Kent State University, Kent, Ohio 44242*

<sup>3</sup>*Institute for Nuclear Research, 47 Prospect Nauki, Kyiv, 03039, Ukraine*

<sup>4</sup>*Dipartimento di Fisica e Ingegneria dei Materiali e del Territorio and Istituto Nazionale per la Fisica della Materia, Università di Ancona, Via Brece Bianche, 60131 Ancona, Italy*

(Received 8 June 2001; published 24 October 2001)

We show that adsorption of dye molecules control the light-induced alignment of dye-doped nematic liquid crystal (LC) on a nonphotosensitive polymer surface. The dependencies of light-induced twist structures on exposure, thermal baking, thickness, and aging before irradiation of the LC cells allowed us to propose the following mechanism for the alignment. Before irradiation, the “dark”-adsorbed layer on the tested surface is formed from dye molecules predominantly aligned along the initial direction of the director. Irradiation of the cell with linearly polarized light produces an additional layer with different orientational ordering of dye molecules. The final easy axis is determined by the competition of “dark” and light-induced contributions to anchoring and is aligned between the “dark” easy axes and polarization of the light. For quantitative interpretation, we apply the tensor model of anchoring and assume that the photoalignment in the mesophase is a cumulative effect of the light-induced anchoring on the background of the already existing anisotropic “dark” dye layer.

DOI: 10.1103/PhysRevE.64.051709

PACS number(s): 61.30.Gd, 68.43.Mn

### I. INTRODUCTION

Effective applications of liquid crystals (LC's) require appropriate alignment. A common alignment technique is a rubbing of polymer surfaces to provide unidirectional orientation of the LC director  $\hat{\mathbf{d}}$ , in a cell [1]. Despite high-quality homogeneous alignment caused by rubbing this method has some deficiencies, e.g., production of electrostatic charges and dust on the surface during treatment. In a developed photoalignment technology [2–5], LC alignment is due to the appearance of an anisotropy axis on a boundary surface irradiated with polarized light. The photoalignment process is a noncontact one and solves the problems associated with rubbing. In addition, it allows effective control of the direction of the easy orientation axis of LC  $\mathbf{e}$  on the aligning surface by changing the direction of the incident light polarization, and the value of the anchoring energy of LC  $W$  by changing the light exposure.

In the traditional photoaligning process an anisotropy axis on an aligning surface is produced with irradiation of the surface before cell assembling. A polarization-sensitive photochemical reaction in an aligning polymer layer is usually responsible for this mechanism of photoalignment [4].

The other photoaligning method is light irradiation of a cell after filling. *In situ* photo-orientation of liquid crystals was first observed in cells filled with dye-doped LC's [6,7]; the method is usually called light-induced LC anchoring [8]. Voloshchenko *et al.* [7] suggested that the easy axis appeared because the light initiated the adsorption of the dye molecules onto the surface.

Our recent studies of light-induced anchoring in the isotropic phase of dye-doped LC [9] has shown that both the

light-induced adsorbed layer and a layer of dark-adsorbed molecules play important roles in the final orientation of the director on the surface. Light irradiation of a cell in the isotropic phase may produce anisotropy in the dark-adsorbed layer either due to photodesorption of molecules or their photoreorientation. As a result, an easy axis perpendicular to light polarization  $\mathbf{E}_{inc}$  appears. At the same time, the direction of easy axis due to light-induced adsorption is parallel to  $\mathbf{E}_{inc}$ , since light-induced adsorption is the most effective for molecules in which long axes are parallel to  $\mathbf{E}_{inc}$ . The resulting  $\mathbf{e}$  is determined by the competition of light-induced adsorption of dye molecules on the substrate and light-induced anisotropy in the dark-adsorbed layer.

The aim of the present paper is to study light-induced anchoring of dye-doped LC in the nematic phase and to clear up a role of the molecular orientational ordering in the mesophase in producing light-induced alignment.

### II. MATERIALS AND BASIC EXPERIMENTS

Light-induced anchoring of pentylcyanobiphenyl (5CB) from BDH Ltd. (clear point,  $T_c = 36^\circ\text{C}$ ) doped with azo-dye methyl red (MR) from Aldridge (weight concentration,  $c = 0.5\%$ ) was examined in a combined cell consisting of the reference and test glass substrates. The reference surface was covered with indium tin oxide (ITO) and rubbed polyimide. The polyimide layer produced strong low-tilted ( $1-2^\circ$ ) planar alignment of 5CB in the direction of the rubbing. The test surface was covered with an ITO layer and an isotropic nonrubbed layer of para-fluoro-poly(vinyl)-cinnamate (PVCN-F). The PVCN-F layer was irradiated with nonpolarized UV light from a Hg lamp (light intensity  $10\text{ mW/cm}^2$ ) for 15 min. This irradiation crosslinked the polymer chains to prevent dissolution of the polymer by 5CB

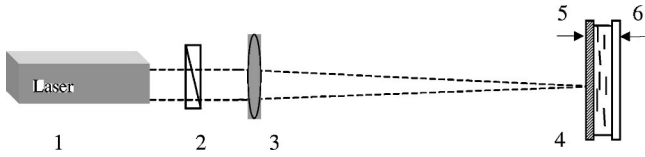


FIG. 1. Experimental setup: (1) He-Cd laser, (2) polarizer, (3) lens, (4) LC cell, (5) tested substrate, and (6) reference substrate.

and to diminish the effect of director slippage over PVCN-F surface [8,10]. Calibrated spacers gave the cell thickness  $L = 45 \mu\text{m}$ . The cell was filled with a mixture of 5CB and MR in the isotropic phase ( $T \approx 70^\circ\text{C}$ ) and cooled down to room temperature in a magnetic field,  $H = 5 \text{ kG}$ , which was parallel to the rubbing direction of the reference surface. The homogeneous planar structure was parallel to the rubbing direction  $\hat{\mathbf{d}}_{ref}$ . The pretilt angle of LC on the tested surface,  $3^\circ$ , was measured with the rotation technique [11].

The cell was placed normal to the incident Gaussian beam of the He-Cd laser (wavelength  $\lambda = 0.44 \mu\text{m}$ , light power  $P < 6 \text{ mW}$ ) (Fig. 1). The beam was focused on the LC layer from the side of the test surface. The diameter (half width of the intensity distribution)  $D$  of the laser beam in the plane of the cell was  $0.25 \text{ mm}$ . The polarization of the incident beam  $\mathbf{E}_{inc}$  was set at a  $45^\circ$  angle to  $\hat{\mathbf{d}}_{ref}$ . The cell was irradiated with different light intensity,  $\bar{I}_{inc} = 4P/\pi D^2$ , during different exposure time,  $t_{exp}$ . The exposure was carried out a day after producing the cell, and the cells were examined in a polarizing microscope a half day after the exposure.

We observed the appearance of structures in the irradiated areas. Analysis of the textures showed that the director on the reference surface was not changed. The twist structures were caused by the reorientation of the director on the tested surfaces  $\hat{\mathbf{d}}_{test}$ , meaning that the stable light-induced easy axis  $\hat{\mathbf{e}}_{test}$  was produced on the tested surfaces.

The dependencies of the twist angle  $\varphi$  between  $\hat{\mathbf{d}}_{test}$  and  $\hat{\mathbf{d}}_{ref}$  on exposure at different intensities  $\bar{I}_{inc}$ , are shown in Fig. 2. At intensities  $\bar{I}_{inc} > 1 \text{ W/cm}^2$ ,  $\varphi$  in the irradiated areas was always positive, i.e., the director turned toward

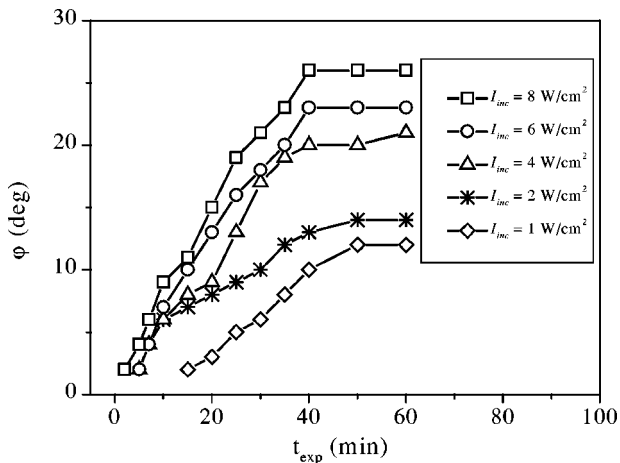


FIG. 2. Twist angle  $\varphi$  vs exposure time  $t_{exp}$  at different intensities.

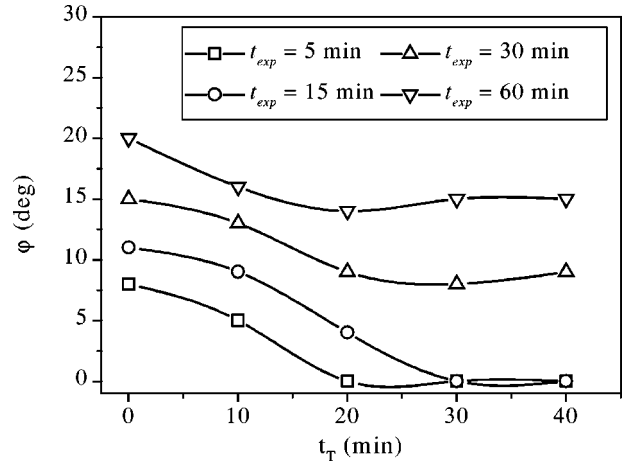


FIG. 3. Twist angle  $\varphi$  vs time of thermal treatment  $t_T$  at different exposure times;  $\bar{I}_{inc} = 5 \text{ W/cm}^2$ .

polarization  $\mathbf{E}_{inc}$ . At the given intensity, the value  $\varphi$  first went up with the exposure and then saturated. The saturated value  $\varphi_{satur}$  increased with the intensity  $\bar{I}_{inc}$  but never achieved  $45^\circ$ , i.e., direction  $\mathbf{E}_{inc}$ .

Experiments at low intensity ( $\bar{I}_{inc} < 1 \text{ W/cm}^2$ ) show poor reproducibility. In most experiments, the director turned toward  $\mathbf{E}_{inc}$ , but sometimes we observed the twist structures with the director being turned outward  $\mathbf{E}_{inc}$  and  $\varphi$  becoming negative. The appearance of the latter abnormal textures was unpredictable. In one of the experiments, we observed two closely located ( $\approx 0.5 \text{ mm}$  distant) textures with opposite signs of the twist angle at the same irradiation parameters. We could not find the conditions necessary for the formation of the abnormal textures. In particular, we did not find correlation between the appearance of these structures and the thickness of the cells, as well as the irradiation parameters (exposure and intensity).

We checked the thermal stability of light-induced anchoring on the tested surface. The cells with the light-induced twist structures obtained at different exposure times, were placed into the hot stage at  $T = 100^\circ\text{C}$  and left for time  $t = 10 \text{ min}$ . Then the cells were slowly cooled to room temperature while in the hot stage, and the light-induced twist structures were compared with the initial ones. This procedure was repeated several times, and the dependence of the twist angle  $\varphi$  on the overall time of keeping the cell at the elevated temperature  $t_T$  was obtained (Fig. 3). The thermal treatment led to the decrease of the twist angle  $\varphi$ . We found a gain in thermal stability of the anchoring with the increase of light exposure. The thermal treatment of the short-exposed cells ( $t_{exp} = 5 \text{ min}$ ) resulted in the complete disappearing of the twist structures after 20 min when keeping the cell at  $T = 100^\circ\text{C}$ . At the longer light exposure ( $t_{exp} = 60 \text{ min}$ ) keeping the cell at  $T = 100^\circ\text{C}$  during the first 10 min caused a small decrease of the value  $\varphi$ ; then the twist structure did not change up to  $t_T = 40 \text{ min}$  of the thermal treatment.

### III. DISCUSSION AND ADDITIONAL EXPERIMENTS

Comparison of the results obtained from irradiation of cells in the mesophase and in the isotropic phase clearly

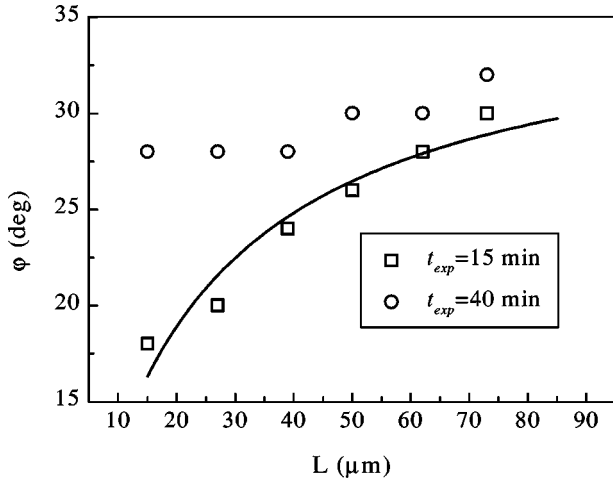


FIG. 4. Twist angle  $\varphi$  vs cell thickness  $L$  at different exposure times;  $\bar{I}_{inc} = 5 \text{ W/cm}^2$ .

demonstrates that orientational order strongly effects the characteristics of light-induced anchoring. In the isotropic phase, the easy axis  $\hat{\mathbf{e}}_{test}$  is either parallel to  $\mathbf{E}_{inc}$  at high intensities or perpendicular to  $\mathbf{E}_{inc}$  at low intensities [9]. In contrast, we found a broad variety of easy axis orientations in the mesophase at low intensities ( $\bar{I}_{inc} < 1 \text{ W/cm}^2$ ). At high intensities, the irradiation never resulted in the orientation  $\hat{\mathbf{d}}_{test}$  along  $\mathbf{E}_{inc}$ .

There can be two reasons why  $\hat{\mathbf{d}}_{test}$  and  $\mathbf{E}_{inc}$  are not parallel. First, the easy axis  $\hat{\mathbf{e}}_{test}$  coincides with  $\mathbf{E}_{inc}$ , but  $\hat{\mathbf{e}}_{test}$  and  $\hat{\mathbf{d}}_{test}$  do not coincide due to the balance of finite anchoring energy on the tested surface  $W$  and the elastic torque  $\sim K_{22}/L$ . Second, the easy axis  $\hat{\mathbf{e}}_{test}$  may not be parallel to  $\mathbf{E}_{inc}$ . To check which situation is realized in our case, we measured the dependence of the twist angle ( $t_{exp} = 15 \text{ min}$ ) on the cell thickness (Fig. 4). This dependence is determined by the torque balance on the tested substrate, which in the Rapini-Papoular approximation for anchoring potential results in

$$\frac{\sin 2(\varphi_0 - \varphi)}{\varphi} = \frac{2K_{22}}{WL}, \quad (1)$$

where  $\varphi_0$  is the twist angle between  $\hat{\mathbf{e}}_{test}$  and  $\hat{\mathbf{d}}_{ref}$ , and  $K_{22} = 3.6 \text{ pN}$  is the twist elastic constant. Fitting experimental data with Eq. (1) allowed us to determine both the anchoring energy value  $W = 0.2 \pm 0.1 \text{ μJ/m}^2$  and  $\varphi_0 = 36.4 \pm 3.5^\circ < 45^\circ$ . Moreover, for the exposure time  $t_{exp} = 40 \text{ min}$  corresponding to the maximum value  $\varphi_{max}$ , (Fig. 4) we also could not reach the value  $45^\circ$ .

Thus, opposite the case of isotropic phase where  $\hat{\mathbf{e}}_{test}$  being either parallel (high-intensity regime) or perpendicular (low-intensity regime) to  $\mathbf{E}_{inc}$ , the irradiation in the mesophase produces  $\hat{\mathbf{e}}_{test}$ , which has intermediate positive position  $\varphi_0 < 45^\circ$ . We believe that the peculiarities of light-induced anchoring in the mesophase are caused by angular ordering of MR and LC molecules. The kinetic theory of

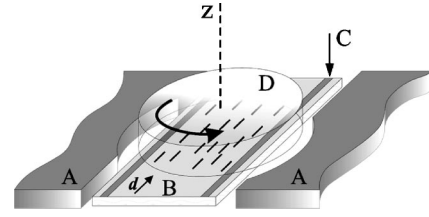


FIG. 5. Experimental setup for measuring of the dependence of the twist angle appeared after rotation of the tested surface on cell age: (A) holder, (B) substrate with the reference surface, (C) spacer, and (D) substrate with the test surface being under mechanical pressure.

light-induced anchoring in the mesophase is a task for additional studies. Below, we consider the main factors that act to produce light-induced easy axis on irradiation in the nematic phase.

The order parameter of MR molecules in 5CB is rather high ( $S_{MR} \approx 0.35$ ) and MR molecules are predominantly oriented parallel to  $\hat{\mathbf{d}}_{test}$  near the tested surface. Therefore, the “dark” adsorption of MR molecules on the tested surface after the cell filling should result in the formation of an anisotropic adsorbed layer and produce “dark” easy axis,  $\hat{\mathbf{e}}_{test}^{dark}$ , parallel to  $\hat{\mathbf{d}}_{ref}$ . To prove this suggestion, we experimented with a combined cell, in which the tested surface could be rotated in the plane of the cell around the  $z$  axis (Fig. 5). The substrate with the test surface coated with a PVCN-F layer was mechanically pressured with spring in order to keep the cell thickness constant. The nominal cell thickness given by spacers glued to the reference surface was  $80 \text{ μm}$ . The cell was filled with the mixture of 5CB and MR in the isotropic state and cooled down to room temperature. After resting for periods ranging from 5 to 300 min, the test substrate was rotated at  $\phi_0 = 90^\circ$  to the direction  $\hat{\mathbf{d}}_{ref}$ ; the value  $L$  varied in the range  $80\text{--}90 \text{ μm}$  during rotation. Analysis of the resulting textures in the polarizing microscope shows that the turning of the test substrates resulted in a twist structure in the cells. The value of the induced twist angle  $\varphi$  was not equal to  $90^\circ$  and depended on cell age before rotation  $t_{age}$ . With increasing  $t_{age}$ , the value  $\varphi$  also increased and saturated to the value  $\varphi_{satur} \approx 70^\circ$  in tens of minutes (Fig. 6). This value cannot be explained by the memory effect [12] because in the cell with pure 5CB, the saturated twist angle is much lower,  $\varphi_{satur} \approx 25^\circ$ . Thus, dark adsorption of MR results in producing the easy axis on the tested surface parallel to  $\hat{\mathbf{d}}_{ref}$ . We estimated the value of the anchoring energy of the “dark” easy axis,  $W_{dark} \approx 0.16 \text{ μJ/m}^2$  by solving Eq. (1) at  $\varphi_{satur} \approx 70^\circ$ ,  $\varphi_0 = \phi_0 = 90^\circ$ , and  $L = 80 \text{ μm}$ . This value, however, is the upper limit of the anchoring induced by dye adsorption, because of the possible memory effect.

Thus, light-induced easy axis is produced on the background of an anisotropic aligning layer with the easy axis  $\hat{\mathbf{e}}_{test}^{dark}$  parallel to  $\hat{\mathbf{d}}_{ref}$  and possessing the anchoring energy  $W_{dark}$ . To describe both dark and light-induced contributions to the anchoring, we use the phenomenological approach, where the dark and light-induced processes are considered as two consecutive aligning treatments. A tensor

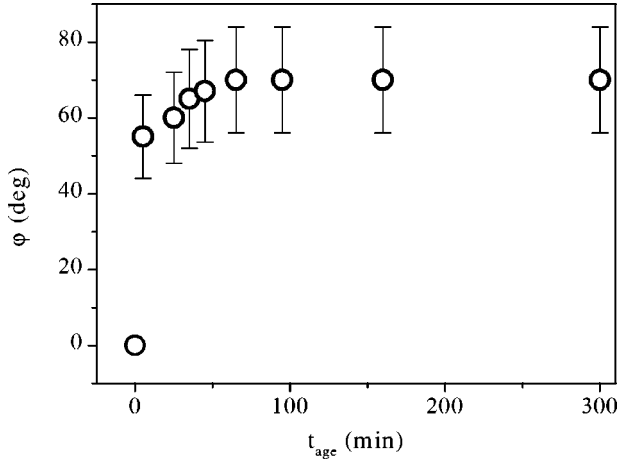


FIG. 6. Twist angle  $\varphi$ , induced by rotation of the tested surface, vs cell age,  $t_{age}$ .

description for the anchoring of LC on the surface exposed to consecutive aligning treatments was recently proposed in [13]. Within this description, the resulting surface energy per unit area is

$$f_s = -\frac{1}{2} \sum_{\alpha, \beta} W_{\alpha\beta} d_{test}^{\alpha} d_{test}^{\beta}, \quad (2)$$

where  $W_{\alpha\beta}$  is the traceless symmetrical anchoring tensor, which is a sum of tensors, that correspond to the different treatments. For planar alignment of LC, the tensor approach describes an azimuthal anchoring in terms of the complex azimuthal anchoring  $\tilde{W} = W \exp(2i\varphi)$ , where  $W$  is a traditional azimuthal anchoring and  $\varphi$  determines the easy axis. The complex description preserves the additivity of different treatments. In our case, the resulting complex anchoring  $\tilde{W}$  on the tested surface is determined by the sum of the initial ‘‘dark’’ anchoring  $\tilde{W}_{dark} = W_{dark} \exp(2i\varphi_{dark})$  and the light-induced anchoring  $\tilde{W}_{hv} = W_{hv} \exp(2i\varphi_{hv})$

$$\tilde{W} = \tilde{W}_{dark} + \tilde{W}_{hv}. \quad (3)$$

To estimate the contribution of the dark anchoring to the total anchoring, we use a graphical representation of the complex anchoring (Fig. 7). The ‘‘dark’’ easy axis  $\hat{\mathbf{e}}_{test}^{dark}$  is formed along the reference rubbing direction,  $\varphi_{dark} = 0$ . The

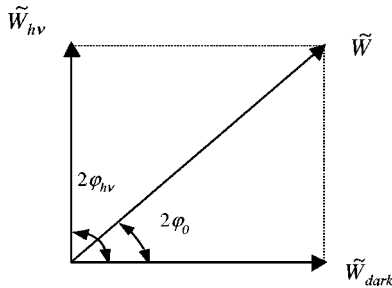


FIG. 7. Graphical representation of the cumulative anchoring [Eq. (3)].

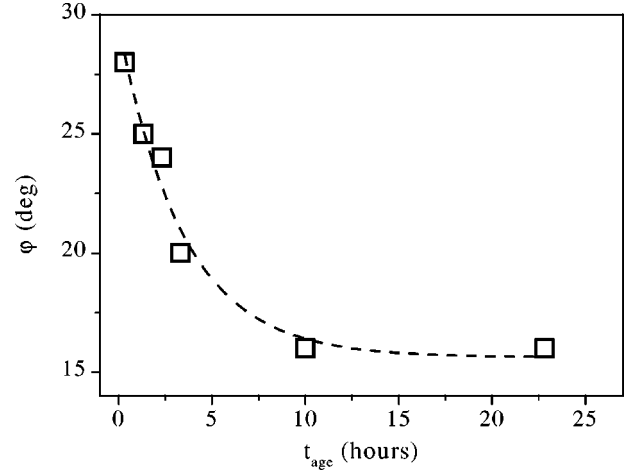


FIG. 8. Twist angle  $\varphi$  vs cell aging time,  $t_{age}$ ;  $\bar{I}_{inc} = 5 \text{ W/cm}^2$ ,  $t_{exp} = 15 \text{ min}$ .

light-induced easy axis  $\hat{\mathbf{e}}_{test}^{hv}$  is parallel to  $\mathbf{E}_{inc}$  and  $\varphi_{hv} = 45^\circ$ . Then, with knowledge of the value  $W = 0.2 \text{ } \mu\text{J/m}^2$  and  $\varphi_0 = 36.4^\circ$  we can estimate the light-induced contribution  $W_{hv} = W \sin(2\varphi_0) = 0.195 \text{ } \mu\text{J/m}^2$  and the dark contribution  $W_{dark} = W \cos(2\varphi_0) = 0.06 \text{ } \mu\text{J/m}^2$  to the total anchoring. The last value is consistent with the upper limit  $W_{dark} \leq 0.16 \text{ } \mu\text{J/m}^2$  estimated from the experiment in the cell with the rotating substrate.

Both experiments and estimations demonstrate that the final orientation of the director on the tested surface depends on the properties of the ‘‘dark’’-adsorbed layer. Below we present the additional experiments where variability of the ‘‘dark’’-adsorbed layer is manifested in the photoalignment.

The irradiation in experiments described above was carried out after the dark-adsorption/desorption processes had reached equilibrium. If the cell age  $t_{age}$  time between filling and irradiation is less than the equilibrium time, the effect of the dark layer should decrease. This conclusion was confirmed by the dependence of  $\varphi$  on  $t_{age}$ , shown in Fig. 8.

It is reasonable to suggest that the increase of MR concentration  $c$  in a bulk should result in a stronger ‘‘dark’’ anchoring, because the amount of adsorbed MR molecules increases on the surface. Therefore, the value  $\varphi$  should decrease with the increase of  $c$ . Actually, we found that the equilibrium value decreases with growing concentration:  $\varphi(c = 0.1\%) \approx 32^\circ$ ,  $\varphi(c = 0.5\%) \approx 26^\circ$ , and  $\varphi(c = 1.5\%) \approx 22^\circ$ .

It is evident that molecular structure and morphology of the adsorbing surface should also strongly affect the characteristics of the dark-adsorbed layer. Voloshchenko *et al.* [7] found that the angle  $\varphi$  could reach  $43^\circ$ , indicating in opposition to our result that the dark-adsorbed layer did not play an essential role in the final anchoring in [7]. This discrepancy may stem from the difference in the aligning materials and their treatments. We used the UV-irradiated para-PVCN-F aligning layer, while a not-irradiated mixture of para- and ortho-PVCN-F was used in [7]. Despite the structural similarity of these materials, they possess different aligning properties, which are strongly changed with UV

treatment [14]. Therefore, the interaction and, in turn, adsorbing affinities of these polymer surfaces are different.

#### IV. CONCLUSIONS

Our studies show that adsorption of dye molecules control the effect of light-induced anchoring at the irradiation of the LC in the nematic phase. Before irradiation, the reference substrate imposes a homogeneous director field in the cell along  $\hat{\mathbf{d}}_{ref}$ . Since the dark-adsorbed layer on the tested surface is formed from dye molecules predominantly aligned along the director, this layer produces the “dark” easy axis parallel to  $\hat{\mathbf{d}}_{ref}$ . Irradiation of the cell with polarized light produces the additional layer with different orientational ordering of dye molecules. The final easy axis is determined by the competition of “dark” and light-induced contributions to anchoring and is aligned between the “dark” easy axes and polarization of the light.

The dependencies of light-induced anchoring on exposure time, concentration of dye, cell age, and temperature confirm the proposed mechanism. For quantitative interpretation, we apply the tensor model of anchoring and consider the photo-alignment in the mesophase as a cumulative effect of the light-induced anchoring on the background of the already existing anisotropic “dark” dye layer. Analysis of experimental thickness dependence of the director alignment on the tested surface after irradiation results in the estimate of the dark anchoring energy  $W_{dark} \approx 0.06 \mu\text{J}/\text{m}^2$ . Direct measurements in the experiment with the rotating substrate give the greater value  $W_{dark} \approx 0.16 \mu\text{J}/\text{m}^2$ . This can be explained in

several ways. First, the memory effect of LC molecules on the tested substrate leads to an overestimation of the dark anchoring energy in the experiment with the rotating substrate. Second, the Rapini-Papoular approximation might deviate from the actual anchoring potential at large deviation angles ( $\approx 20^\circ$ ). Third, the light-induced layer is adsorbed onto the dark layer, screening the action of the dark layer on LC alignment. Quantitative description of the screening effect requires the kinetic model of adsorption/desorption flows of orientationally ordered dye molecules. The isotropic version of the kinetic model has been developed [15]. If the irradiation intensity is strong enough, the model should also take into account self-consistent interaction between director field and polarization characteristics of propagating light [10,16,17]. Fortunately, in our experiments, the dark layer prevented the sliding of the director on the surface, and the orientational diffusion of dye molecules diminished the effect, of bulk director photoreorientation on the orientation of adsorbed molecules.

#### ACKNOWLEDGMENTS

The authors are very thankful to A. Iljin, O.D. Lavrentovich, and S. Slussarenko for useful discussions. The research was supported by CRDF Grant No. UP1-2121A, NSF ALCOM Grant No. DMR 89-20147, INTAS YSF Grant No. 00-4178 (E. Ouskova), Grant No. B29/13 of the Fund of the Academy of Sciences of Ukraine, and INCO Copernicus Concerted Action “Photocom” (EC Contract No. ERB IC15 CT98 0806).

- 
- [1] L.M. Blinov, E.I. Kats, and A.A. Sonin. *Usp. Fiz. Nauk* **152**, 449 (1987) [*Sov. Phys. Usp.* **30**, 604 (1987)].
- [2] W.M. Gibbons, P.J. Shannon, S.T. Sun, and B.J. Swetlin. *Nature (London)* **351**, 49 (1991).
- [3] A.G. Dyadyusha, T. Ya. Marusii, V. Yu. Reshetnyak, Yu. A. Reznikov, and A.I. Khizhnyak. *Pis'ma Zh. Éksp. Teor. Fiz.* **56**, 18 (1992) [*JETP Lett.* **56**, 17 (1992)].
- [4] M. Schadt, K. Schmitt, V. Kozenkov, and V. Chigrinov. *Jpn. J. Appl. Phys., Part 1* **31**, 2155 (1992).
- [5] F. Simoni and O. Francescangeli, *J. Phys.: Condens. Matter* **11**, R439 (1999).
- [6] S.T. Sun, W.M. Gibbons, and P.J. Shannon, *Liq. Cryst.* **12**, 869 (1992).
- [7] D. Voloshchenko, A. Khizhnyak, Yu. Reznikov, and V. Reshetnyak. *Jpn. J. Appl. Phys., Part 1* **34**, 566 (1995).
- [8] O. Francescangeli, S. Slussarenko, F. Simoni, D. Andrienko, V. Reshetnyak, and Yu. Reznikov *Phys. Rev. Lett.* **82**, 1855 (1999).
- [9] E. Ouskova, D. Fedorenko, Yu. Reznikov, S.V. Shiyankovskii, L. Su, J.L. West, O.V. Kuksenok, O. Francescangeli, and F. Simoni. *Phys. Rev. E* **63**, 021701 (2001).
- [10] T. Marusii, Yu. Reznikov, and S. Slussarenko *Mol. Mater.* **6**, 163 (1996).
- [11] G. Baur, V. Wittner, and D.W. Berreman, *Phys. Lett.* **56A**, 142 (1976).
- [12] P. Vetter, Y. Ohmura, and T. Uchida. *Jpn. J. Appl. Phys., Part 2* **32(9A)**, L1239 (1992).
- [13] S.V. Shiyankovskii, A. Glushchenko, Yu. Reznikov, O.D. Lavrentovich, and J.L. West, *Phys. Rev. E* **62**, R1477 (2000).
- [14] D. Andrienko, A. Dyadyusha, Yu. Kurioz, Yu. Reznikov, F. Barbet, D. Bormann, M. Warenghem, and B. Khelifa. *Mol. Cryst. Liq. Cryst.* **329**, 831 (1999).
- [15] O.V. Kuksenok, and S.V. Shiyankovskii, *Mol. Cryst. Liq. Cryst.* **329**, 831 (2001).
- [16] I. Jánossy and L. Szabados *Phys. Rev. E* **58**, 4598 (1998).
- [17] D. Andrienko, V. Reshetnyak, Yu. Reznikov, and T.J. Sluckin. *Phys. Rev. E* **63**, 011701 (2001).